Modeling the effect of anisotropy on TCV equilibria using the MEQ suite of codes

G. Van Parys[1], A. Merle[1] and J. P. Graves[1]
[1] *Swiss Plasma Center (SPC), EPFL, Lausanne, Switzerland*

With the recent installation of a second tangential Neutral Beam Injection (NBI) system on the Tokamak à Configuration Variable (TCV) [1], higher ratios of fast ions to bulk pressures, and therefore pressure anisotropy are expected. This paper shows the implementation of these effects in the Matlab EQuilibrium (MEQ) suite of codes [2], the benchmark of the updated code against analytical estimates as well as against the ANIMEC code [3] followed by the demonstration that this new physics impacts the reconstruction of the total plasma energy via the analysis of a TCV discharge.

The MEQ suite with anisotropy MEQ is the suite of free-boundary axisymmetric equilibrium codes which was originally developed for TCV discharge planification and analysis and has been adapted to other machines. For the modelling of the hot ions, we use a distribution function compatible with their approximate constants of motion, in the limit of zero orbit width. A particularly convenient choice is the modified bi-Maxwellian [4]:

$$f_h(\psi,\mathcal{E},\mu)=\frac{m_h^{3/2}n_c(\psi)}{(2\pi)^{3/2}T_\perp(\psi)T_\parallel(\psi)^{1/2}}\exp\left[-\left(\frac{\mu B_c(\psi)}{T_\perp(\psi)}+\frac{|\mathcal{E}-\mu B_c(\psi)|}{T_\parallel(\psi)}\right)\right] \tag{1}$$

Which is parametrized by the profiles $\left\{n_c(\psi),B_c(\psi),T_\parallel(\psi),T_\perp(\psi)\right\}$ allowing for great flexibility in the modeling. B_c is usually taken to be constant and is physically interpreted as the value of the magnetic field where the ion cyclotron resonance condition is verified. From moments of this distribution, one obtains the pressures as functions of the poloidal flux ψ and the magnetic field strength B acting as equations of state for the plasma [3]:

$$p_\parallel(\psi,B):=p_{th}(\psi)(1+p_h(\psi)H(\psi,B)),\qquad p_\perp(\psi,B)=p_\parallel(\psi,B)-B\left(\frac{\partial p_\parallel}{\partial B}\right)_\psi \tag{2}$$

Where the second equation is obtained from the projection of the force balance equation in the ∇B direction. The generalized toroidal field flux function and the generalized Grad-Shafranov Equation (GSE) are obtained respectively from projections of the force balance equation in the $\nabla\phi$ and the $\nabla\psi$ directions:

$$B=\nabla\phi\times\nabla\psi+g\nabla\phi,\qquad \sigma_\parallel:=\mu_0\frac{p_\parallel-p_\perp}{B^2},\qquad T(\psi)=(1-\sigma_\parallel)g \tag{3}$$

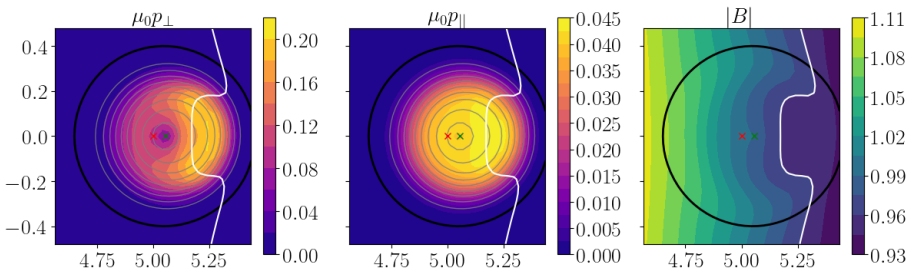

Figure 1: Parallel and perpendicular pressure fields, showing their respective poloidal dependence, and magnetic field strength, showing the diamagnetism of the plasma, for the analyzed scenario.

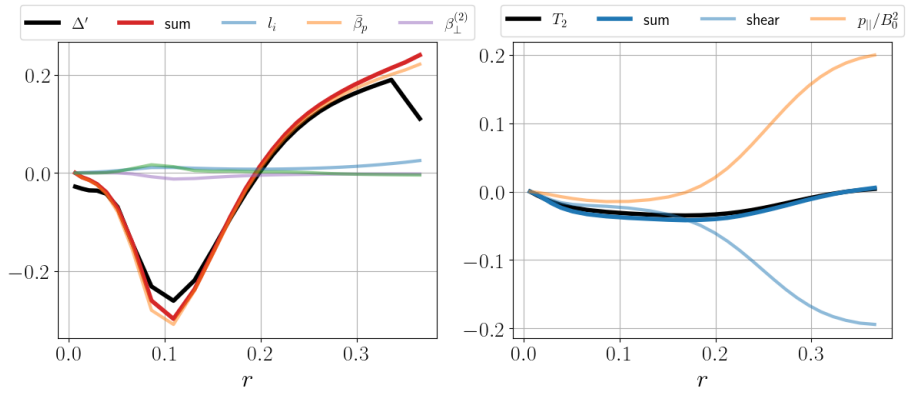

Figure 2: Radial derivative of the Shafranov Shift Δ', compared to the prediction of Eq.(5), with all contributions separated (left). Toroidal flux function $T - R_0 B_0$ compared to theoretical prediction in Eq.(4) (right).

The free flux functions describing the equilibrium are: $\{p_{th}(\psi), T(\psi), p_h(\psi), T_\perp/T_\parallel(\psi)\}$. The forward problem is solved with an updated version of the FGS [2] code, in which the magnetic field strength is added to the state vector: $\boldsymbol{x} = \{\psi, B\}$. The reconstruction problem is solved using LIUQE [5], which uses a Picard iteration scheme in which we use the previous iteration's value of the magnetic field strength B to compute the terms appearing in the GSE. The expression of the diamagnetic loop measurement is modified according to the modification to the toroidal field in Eq.(3).

Benchmarking of the code We use the local inverse aspect ratio expansion as in [6], we quote here the two results that are verified in the code FGS in Figs.(1) and (2) (here (r, ω) are flux coordinates for which Eqs.(20-21) of [6] are verified):

$$\left(T(r) + \frac{\bar{p}_\parallel}{B_0^2}\right)' = \frac{1}{2r^2}\left(r^2 \psi'^2\right)' \tag{4}$$

$$\Delta'(r) = \frac{r}{R_0}\left(\bar{\beta}_p(r) + \frac{l_i(r)}{2} + \beta_\perp^{(m=2)}(r) + \gamma_\perp^{(m=2)}(r)\right) \tag{5}$$

which correspond to Eqs.(25) and (29) in the reference. The equilibrium is shown in Fig.(1), and the comparison between simulation and predictions is shown in Fig.(2). Next, we benchmark the updated FGS code against ANIMEC, with test case similar to the one shown in [3], i.e.

Figure 3: Comparison of ANIMEC (left) and MEQ (right) on the highly poloidally dependent perpendicular pressure $p_\perp$ as well as of the magnetic field strength B on a High Field Side ICRH heated scenario

Figure 4: Comparison of ANIMEC (left) and MEQ (right) on the highly poloidally dependent perpendicular pressure $p_\perp$ as well as of the magnetic field strength B on a Low Field Side ICRH heated scenario

constant anisotropy $T_\perp/T_\parallel = 3$ and hollow hot ion profile $p_h(\hat{\psi}) = 4\hat{\psi}(1-\hat{\psi})$ with $\hat{\psi}$ the normalized poloidal flux. Extremely good agreement is shown for the poloidal dependence of the perpendicular pressure and on the plasma diamagnetism. in Figs.(3) and (4).

Coupling with ASTRA and TCV discharge analysis The updated version of LIUQE is coupled to the ASTRA code via adaptations of formulas appearing in [7] (Section 7.4). The resulting profiles are shown in Fig.(5) for TCV discharge #81331, where we observe a significant parallel anisotropy that is consistent with a parallel injection. We also note that in some region, the pressure of the hot ions is comparable to the bulk pressure. Fig.(6) shows the comparison of the inferred total plasma energy between LIUQE with the hot ion profiles from Fig.(5) and without them (i.e. isotropic LIUQE), with given diamagnetic signal Φ_p to which we give an important weight, by setting its uncertainty to $\Delta\Phi_p = 10^{-1}$ mWb in LIUQE, to show that this magnetic measurement strongly constrains the total perpendicular plasma energy (electrons,

Figure 5: Radial profiles of the hot ions' flux functions obtained from fitting ASTRA results on shot #81331 from $t \in [0.9; 1.5]$ s while Neutral Beam Injection is turned on.